

NUMERICAL SIMULATION OF RIDGE ICE AND AERODYNAMIC EFFECT UNDER THERMAL ANTI-ICE

Guo LingBo¹, Cao GuangZhou², Zhang HuiPing¹

¹Shanghai Aircraft Design and Research Institute
²Nanjing University of Aeronautics and Astronautics

Abstract

Under the condition of thermal anti-icing, the liquid water on the leading edge of the airfoil would flow to the downstream non-protective zone will produce ridge ice, thus endangering flight safety. Based on the existing three-dimensional (3D) icing model which considers the water film flow on the ice layer, the influence of evaporation on the ice accretion process is considered, and the evaporation and the surface temperature of water film are coupled. Under the condition of thermal anti-ice, the mathematical model and calculation method of the three-dimensional icing model are developed. In this paper, the ridge ice on the airfoil are simulated and compared with experimental results, the rationality of the three-dimensional icing model is validated. The numerical results show that with the increase of heat flux, the ice shape on the airfoil gradually transitions from glaze ice to ridge ice. Furthermore, both glaze ice and ridge ice would decrease the lift and increase the drag. And compared to the glaze ice, the ridge ice is more harmful.

Keywords: thermal anti-ice, ridge ice, water film flow, water film evaporation, aerodynamic characteristics

1. Introduction

When airplanes pass through clouds which contain supercooled water droplets, ice will accrete on the surfaces of the upwind components. Ice reduces the lift as much as 35% [1], and the drag can be increased by three times compare with a smooth airfoil.

Ice accretion caused by supercooled water droplets first occurs on the leading edge of the component [2]. Due to the different environmental conditions of ice accretion, it mainly consists of rime ice and glaze ice [3]. Rime ice is loose and the ice shape is closer to the aerodynamic shape. Glaze ice is firm and behaves double horn shape, so the impact on the flight performance is more serious. In order to reduce the danger of ice accretion, heat flux is generally provided to the front ice accretion zone. On this occasion, the water film would flow downstream and freeze to ridge ice. Research shows that ridge ice has serious influence on the aerodynamic performance of airfoil [4]. So the study on ridge ice is very important to flight performance and safety.

2. Mathematical Model and Calculation Method for Ridge Ice Accretion

2.1 Assumptions

According to the characteristics and complexity of 3D ice accretion, the assumptions are proposed as follow:

- 1) The incoming flow condition is assumed to be constant.
- 2) The thermophysical properties of air and supercooled water are assumed to be constant. Once the water film is freezing, the thermophysical properties change to be the same as ice instantly.
- 3) The surface tension of the water film and the influence of the water droplets impact are ignored. The water film is considered to be laminar flow.
- 4) The convection term in the film heat transfer equation is ignored.
- 5) The roughness of the airfoil surface is assumed to be constant.
- 6) The influence of water droplets on the lift coefficient is ignored.

2.2 Mathematical Model

The control volume of ice accretion is shown in Fig.1. There are three layers from top to bottom:

air-supercooled water droplets flow, thin water film flow and ice layer.

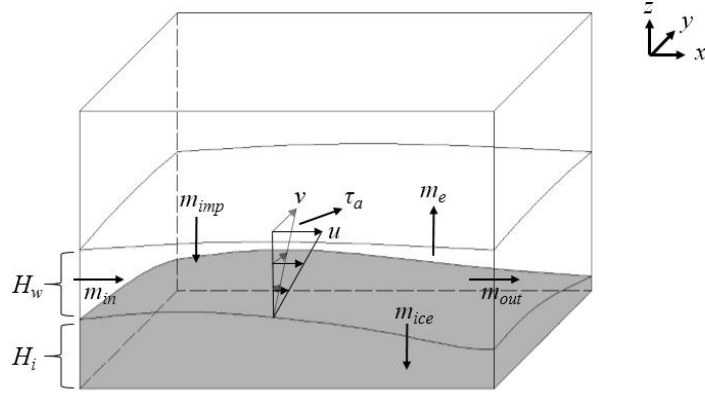


Fig. 1 Mathematical model

The flow of the thin water film directly affects the ice accretion. In Fig.1: m_{in} is the mass flux of supercooled water from the previous control volume; m_{out} is the mass flux of water flow into the next control volume; m_e is the mass flux of water evaporated with the air; m_{ice} is the mass flux of supercooled water frozen to ice; H_w is the thickness of the water film; u and v are the flow speeds of the water film in x and y directions respectively; H_i is the thickness of ice layer. Based on the icing model in the Ref. [5], the mathematical model which consider the influence of evaporation on the ice accretion process is developed, which contains seven equations as follows: mass equation, momentum equations, energy equations, and the stefan equation.

$$\frac{\partial H_w}{\partial t} + \frac{\partial}{\partial x} \left(\int_0^{H_w} u dz \right) + \frac{\partial}{\partial y} \left(\int_0^{H_w} v dz \right) = \frac{m_{imp}}{\rho_w} - \frac{m_e}{\rho_w} - \frac{\rho_i}{\rho_w} \frac{\partial H_i}{\partial t} \quad (1)$$

$$-\frac{1}{\rho_w} \frac{\partial p}{\partial x} + g_x + \nu \frac{\partial^2 u}{\partial z^2} = 0 \quad (2)$$

$$-\frac{1}{\rho_w} \frac{\partial p}{\partial y} + g_y + \nu \frac{\partial^2 v}{\partial z^2} = 0 \quad (3)$$

$$\frac{\partial p}{\partial z} = 0 \quad (4)$$

$$\frac{\partial}{\partial z} \left(\frac{\partial T_w}{\partial z} \right) = 0 \quad (5)$$

$$\frac{\partial}{\partial z} \left(\frac{\partial T_i}{\partial z} \right) = 0 \quad (6)$$

$$\frac{\partial H_i}{\partial t} = \frac{1}{\rho_i L_f} \left(\lambda_i \frac{\partial T_i}{\partial z} - \lambda_w \frac{\partial T_w}{\partial z} \right) \quad (7)$$

Eqs.(1)-(4) are the flow equations of unfrozen thin water film. Eq.(5) and (6) are the energy equations of water film layer and ice layer. Eq.(7) is the growth rate equation for ice layer. In these equations, ρ_i and ρ_w are the density of ice and water respectively; λ_i and λ_w are the thermal conductivity of ice and water; ν , g and L_f are the dynamic viscosity, acceleration of gravity and latent heat of solidification respectively.

2.3 Calculation Method of Evaporation

When the air flow over the surface of the water film, the temperature on the surface of the water film is higher than the boundary layer of the air flow, it causes a higher concentration flow field of water vapor close to the water film, which allows the water molecules diffuse into the air flow. The water molecules continuously absorb the heat and move outward from the surface of the water

film, It means the mass transfer and heat transfer occurs at the same time. According to Ref.[6], the mass transfer is similar to the convective heat transfer, and the evaporation capacity can be described as follows:

$$m_e = \frac{hM_w}{\rho_a c_{pa} R} \left[\frac{P_{sat}(T_w|_{z=H_w})}{T_w|_{z=H_w}} - \frac{P_{sat}(T_\infty)}{T_\infty} \right] \quad (8)$$

In the Eq.(8), h is the convective heat transfer coefficient between the surface of water film and air flow, ρ_a and c_{pa} are the density and the specific heat at constant pressure of the air flow respectively, M_w is the molar mass of the water molecule, T is the steam temperature, R is the universal gas constant, $R=8.315\text{kJ}/(\text{kmol}\cdot\text{k})$ in this paper, $P_{sat}(T)$ is the saturated vapor pressure at the steam temperature T . According to Ref.[7], the saturated vapor pressure $P_{sat}(T)$ can be described as follows:

$$P_{sat}(T) = \frac{10^{33.59051+0.0024804T-\frac{3142.31}{T}}}{T^{8.2}} \quad (9)$$

2.4 Boundary Conditions

The boundary conditions for Eqs.(2)-(4) are the same with that in Ref.[5]. And the boundary conditions for Eq.(5) as follows:

$$T_w|_{z=0} = T_f \quad (10)$$

$$-\lambda_w \frac{\partial T}{\partial z} \Big|_{z=H_w} = h[T_w|_{z=H_w} - T_a] - \frac{1}{2} m_{imp} U_\infty^2 + m_{imp} c_{pw} [T_w|_{z=H_w} - T_\infty] + m_e L_e \quad (11)$$

T_f is the water freezing temperature, and C_{pw} is the constant-pressure specific heat capacity of water in these equations.

Without heat flux in the leading edge area, glaze ice accretion occurs. The boundary conditions for Eq. (6) as follows:

$$T_i|_{z=0} = T_f \quad (12)$$

$$\lambda_i \frac{\partial T_i}{\partial z} \Big|_{z=-H_i} = 0 \quad (13)$$

When heat flux is introduced in the leading edge area, the glaze ice layer will be thinner. And the unfrozen water film will flow to downstream and freeze to the ridge ice, the Eq. (13) in the heating region is modified as follows:

$$\lambda_i \frac{\partial T_i}{\partial z} \Big|_{z=-H_i} = Q \quad (14)$$

Q is the heat flux transferred to the control volume, which is provided by anti-ice system, According to the energy conservation equation, Q can be described as follows:

$$-Q_{imp} + Q_{cp} + Q_h + Q_e - Q_{ice} = Q \quad (15)$$

Q_{imp} is the kinetic energy of the supercooled water droplets, Q_{cp} is the energy required for heating the supercooled water droplets to the temperature of the water film, Q_h is the convective heat transfer energy exchanged between the water film surface and the air/supercooled flow, Q_e is the energy exchanged on the surface of the water film due to evaporation, Q_{ice} is the latent heat released during ice accumulation, and each item can be described as follows:

$$Q_{imp} = \frac{1}{2} m_{imp} U_\infty^2 \quad (16)$$

$$Q_{cp} = m_{imp} c_{pw} [T_w|_{z=H_w} - T_\infty] \quad (17)$$

$$Q_h = h [T_w|_{z=H_w} - T_a] \quad (18)$$

$$Q_e = m_e L_e \quad (19)$$

$$Q_{ice} = m_{ice} L_f \quad (20)$$

L_e is the latent heat coefficient of vaporization when the water film evaporated, U_∞ and T_∞ are the velocity and temperature of the incoming air/supercooled flow respectively. T_a is the temperature of the air/supercooled flow close to the surface of the water film.

When the Q is large enough, Q_{ice} would be less than 0 according to Eq. (15), which indicates that the water film would be maintained in this case. At this time, Eq. (6) should be ignored, and the boundary condition Eq. (10) should be modified as follows:

$$-\lambda_w \left. \frac{\partial T}{\partial z} \right|_{z=0} = Q \quad (21)$$

At this time, boundary conditions Eq. (11) and Eq. (21) should be used to calculate Eq. (5), and the surface temperature of the water film can be obtained as follows:

$$T_w \Big|_{z=H_w} = \frac{Q_{si} + 0.5m_{imp}U_\infty^2 + hT_a + m_{imp}c_{pw}T_\infty - m_e L_e}{h + m_{imp}c_{pw}} \quad (22)$$

Eq.(8) and Eq.(22) describe the calculation equations of evaporation and water film surface temperature respectively, which indicates that the two parameters are coupled and constitute a transcendental equation. Therefore, the dichotomous method is used in this paper, and the numerical solutions of water film surface temperature and evaporation mass would be obtained through iteration.

Also, from the mathematical model of ice accretion, H_w , H_i , T_w and T_i are coupled with each other. However, when Q is given, it is possible to obtain H_i first from Eq.(7). And then all the equations are solved orderly[5].

3. Simulation and Analysis

In this paper, ANSYS-CFX is used to calculate the air-water droplets flow around the airfoil. The continuous -discrete fluid model based on Euler-Euler method is used. The air is set as continuous fluid phase, while the water droplets is set as discrete fluid phase. The sum of the volume fractions of air and water droplets is 1. Flow turbulence is treated by $k-\varepsilon$ turbulence model.

The lift and drag of airfoil are calculated by ANSYS-FLUENT. Since the velocity of incoming flow is low, pressure-based solver is used and the flow turbulence is also treated by $k-\varepsilon$ turbulence model.

3.1 Ridge Ice Simulation

In this paper, NACA23012 is selected for ridge ice simulation. The calculation area is shown in Fig.2. The upstream area is set as a semicircular region with radius of $6c$, while the downstream area is set as $8c \times 12c$ rectangular region. The surface "wall" (airfoil and fuselage) is set as non-sliding. The surface "In" (surfaces upstream the airfoil) is set as velocity-inlet. the surface "symmetry" is set as symmetry condition. The surface "out" (surface downstream the airfoil) is set as pressure outlet. The parameters of the airfoil and computational conditions are shown in Table1:

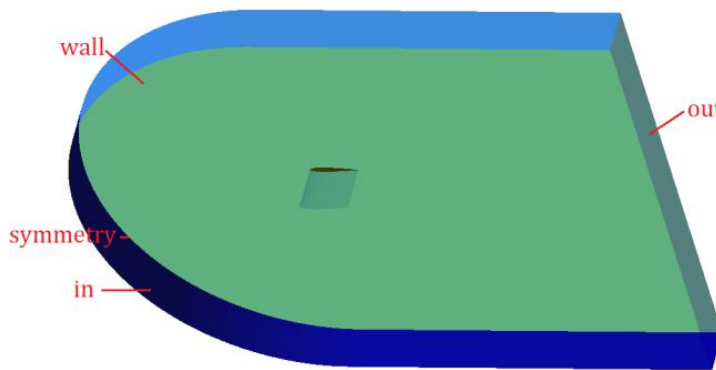


Fig. 2 Calculation area

Table 1 Computational conditions of ridge ice simulation

<i>chord</i> (m)	<i>AOA</i> (°)	U_{∞} (m/s)	T (K)	LWC (g/m ³)	MVD (μm)	<i>Icing time</i> (s)
0.46	0.9	90.05	264.65	0.64	15	300

Hexahedral structured mesh is generated by ANSYS-ICEM. The air/supercooled flow and the lift/drag are both simulated on this mesh. The water film flow and ice accretion are both calculated in the first layer mesh. Thus the mesh near the wall should be dense and well-orthogonal. The mesh used in this paper is shown in Fig.3. The height of the first layer mesh is about 0.1mm. The growth factor is set as 1.2. The first layer mesh shows good orthogonality to the airfoil surface.

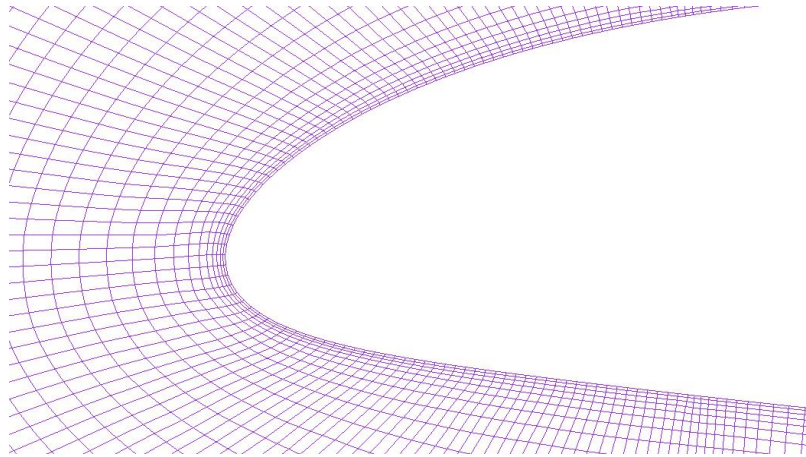


Fig. 3 Mesh near the airfoil

The simulation for 3D ice accretion can be mainly divide into five parts:(1) physical modeling and meshing, (2) air/supercooled flow simulation, (3) water droplet impingement calculation, (4) ice accretion and water film flow simulation, (5) ice layer shape and mesh reconstruction. The total ice accretion time is 300s. During the process of simulation, the meshing and the caculation for two-phase flow are updated every 60 seconds. The lift and drag can be obtained after the ice layer shape is updated.The re-meshing result for the iced airfoil is shown in Fig.4.

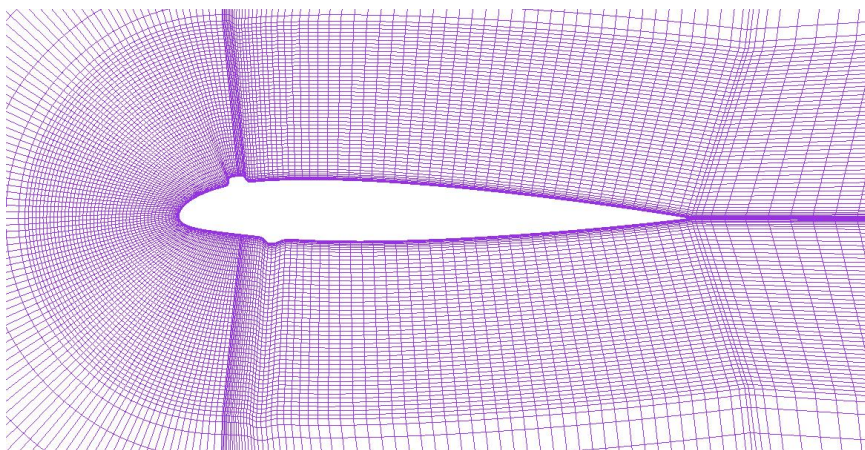


Fig. 4 Re-meshing result for the iced airfoil(icing time is 300s)

The ridge ice on the NACA23012 airfoil is simulated to validate the rationality of the 3D icing model developed in this paper. The physical model and computational parameters (as shown in Table 1) are the same as the example in reference [8], and the comparisons are shown in Fig.5.

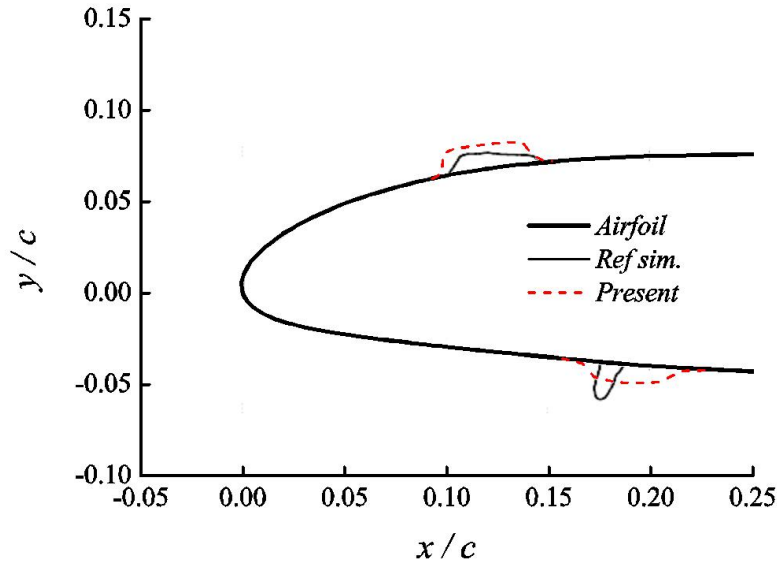


Fig. 5 Comparison results

Fig.5 shows that the volume of the ice accretion simulated in this paper are close to the results in Ref. [8], and the shape of the ridge ice on the upper surface of the airfoil is similar to the experimental results. However, on the lower surface of the airfoil, the coverage area of simulation result is larger while the height is lower .

Fig.6 shows the shape of the ridge ice on the surface in the experimental results. On the lower surface of the airfoil, different shapes of ice are occurred on different sections, thus it is difficult to simulate the shape accurately.

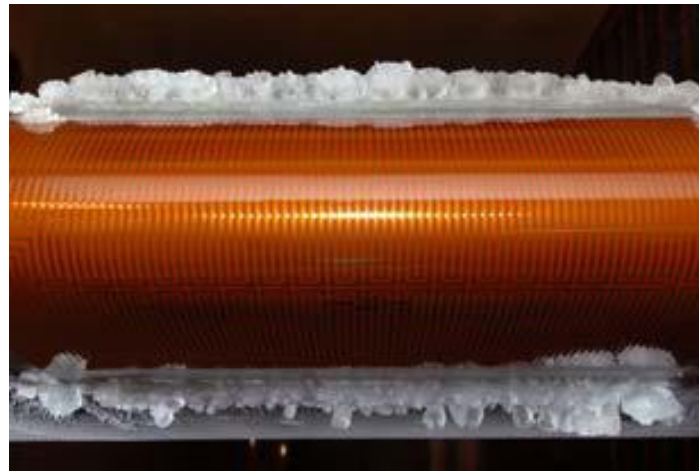


Fig. 6 Experimental results in Ref.[8]

3.2 Contrast Between Glaze Ice and Ridge Ice

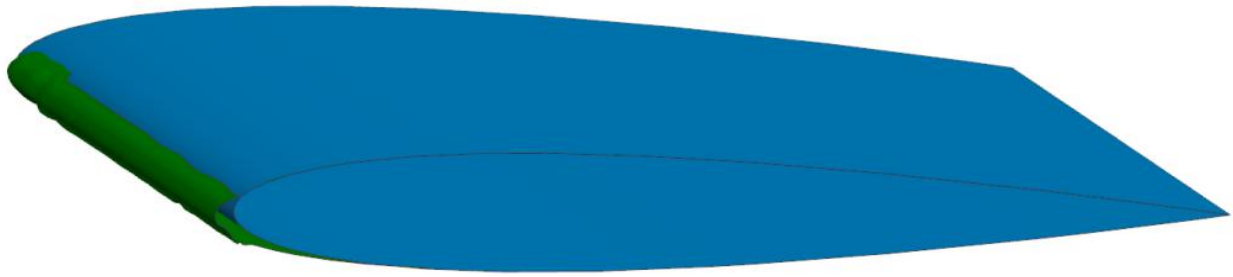
Based on the mathematical model developed in this paper, the shapes of ice under different anti-icing heat fluxes can also be obtained, which leads to different aerodynamic effects. NACA0012 is selected for this simulation, the calculation area and the method of meshing and calculating are the same as the previous section, the parameters of the airfoil and computational conditions are shown in Table 2.

Table 2 Computational conditions

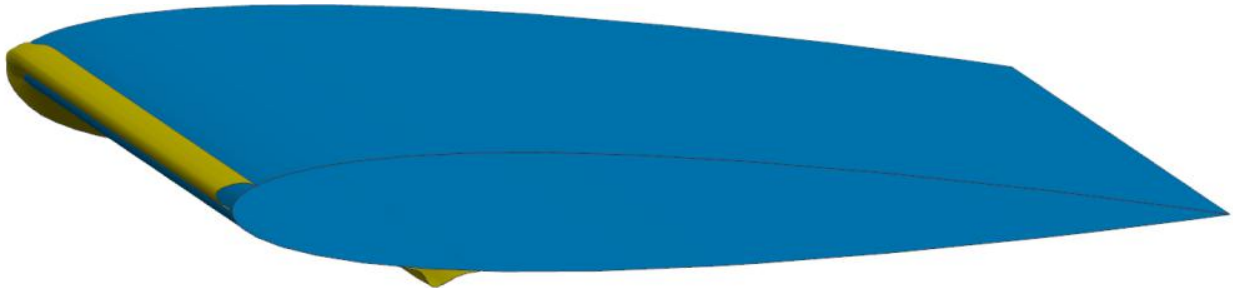
<i>chord</i> (m)	<i>AOA</i> (°)	U_{∞} (m/s)	<i>T</i> (K)	<i>LWC</i> (g/m ³)	<i>MVD</i> (μm)	<i>Icing time</i> (s)
0.3	4	129.46	260.55	0.5	20	120

The anti-icing heat flux Q is added to the impact area of the supercooled water droplets. In the process of Q increasing from 0 to 160 gradually, it is transitioned from glaze ice to ridge ice on the surface of airfoil, and the ice disappeared eventually. During the continuous transition process, three

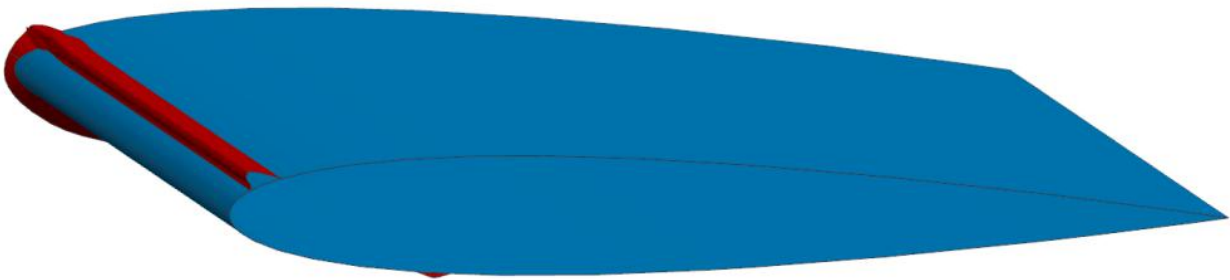
thermal anti-icing conditions is chose in this paper, while Q is set to be 0kW/m^2 , 30kW/m^2 , and 60kW/m^2 , the three-dimensional ice shapes of glaze ice, transitional ice and ridge ice are showed in Fig.7, in order to reduce the influence of the boundary effect, the two-dimensional ice shapes of the middle section on the airfoil are extracted.



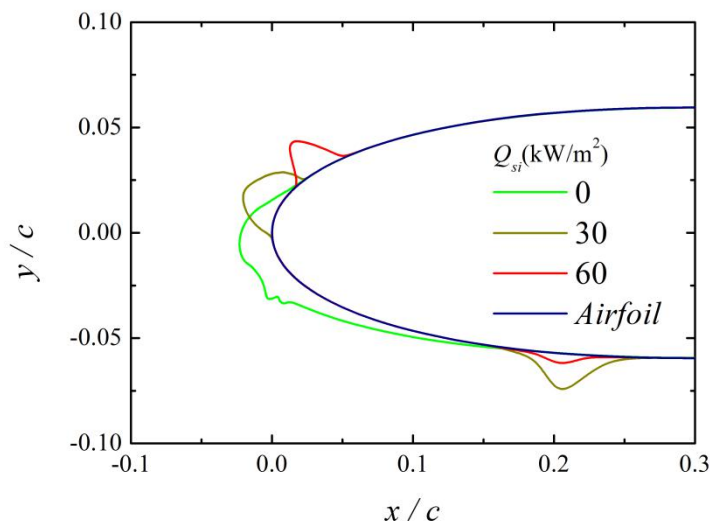
(a) three-dimensional ice shape($Q=0\text{kW/m}^2$)



(b) three-dimensional ice shape($Q=30\text{kW/m}^2$)



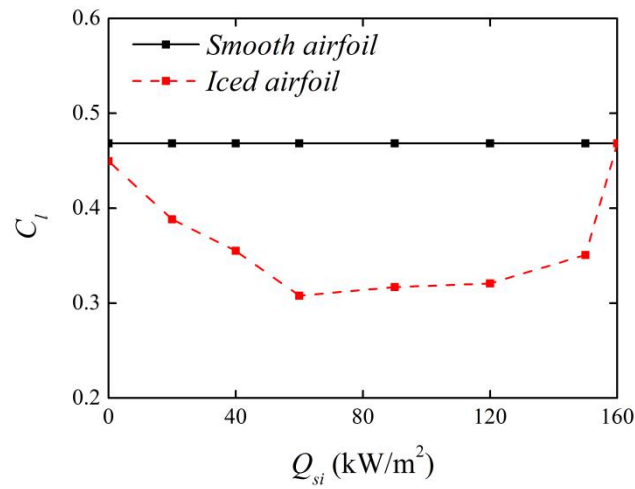
(c) three-dimensional ice shape($Q=60\text{kW/m}^2$)



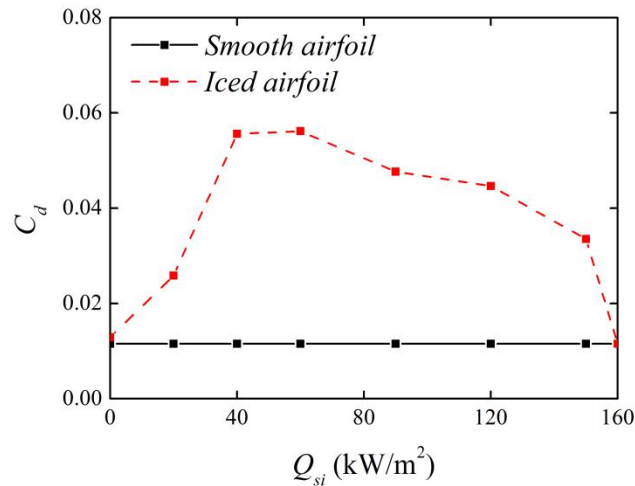
(d) two-dimensional ice shapes under different heat flux

Fig. 7 Ice shapes under different heat flux

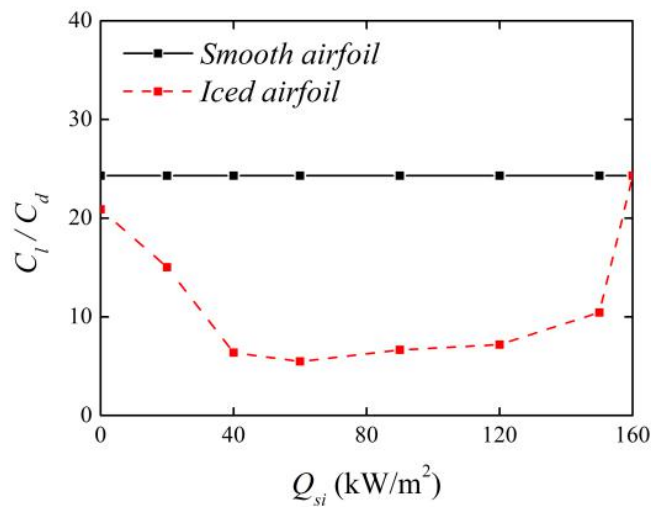
As the anti-icing heat flux increases, the lift coefficient, drag coefficient and lift-to-drag ratio under different ice shapes are showed in the Fig.8.



(a) lift coefficient to heat flux



(b) drag coefficient to heat flux



(c) lift-to-drag ratio to heat flux

Fig. 8 The aerodynamic performance under different heat flux

While the Q is 0kW/m^2 , glaze ice occurs on the surface of the airfoil, and the lift coefficient of the iced airfoil decreases while the drag coefficient increases. During Q increases to 60kW/m^2 , the glaze ice transitions to ridge ice gradually, and the aerodynamic performance become worsen, the largest thickness of ridge ice would be occurred while the Q is 60kW/m^2 , at this time, the lift coefficient of the iced airfoil is reduced to the minimum. While the Q increases from 60kW/m^2 to 160kW/m^2 , the thickness of the ridge ice decreases gradually, the lift coefficient increases while the drag coefficient decreases. While the Q is higher than 160kW/m^2 , the ridge ice is disappeared and only water film exists on the surface of airfoil, the aerodynamic performance is the same as a smooth airfoil.

From the variation process of aerodynamic performance, it indicates that while the anti-ice heat flux gradual increase, the aerodynamic performance of the iced airfoil may become worsen, thus the protective area and the heat flux should be reasonably arranged in the anti-icing design.

4. Conclusion and suggestion

Based on the 3D icing model established in Ref. [5], the influence of evaporation on the ice accretion process is considered, the ridge icing model and its calculation methodology are developed. Under the thermal anti-icing condition, the glaze ice accretion and ridge ice accretion are simulated, the lift coefficient and drag coefficient are compared to the smooth airfoil. Some results are concluded as follows:

- (1) Based on the 3D icing model and its calculation methodology developed in Ref. [5], ridge ice accretion can be simulated by introducing the calculation of evaporation.
- (2) When the heat flux for anti-icing is introduced, some water film would flow from the leading edge to the downstream area, so glaze ice and ridge ice are both occurred.
- (3) Compared to the smooth airfoil, both glaze ice and ridge ice would decrease the lift and increase the drag.
- (4) While the anti-ice heat flux is used, the aerodynamic performance of the iced airfoil may become worsen, thus the protective area and the heat flux should be reasonably arranged in the anti-icing design.

References

- [1] Potapczuk M G, Berkowitz B M. Experimental investigation of multielement airfoil ice accretion and resulting performance degradation [J]. *Journal of Aircraft*, 1990, 27 (8): 679-691.
- [2] Kind R J, Potapczuk M G, Feo A, et al. Experimental and computational simulation of in-flight icing phenomena [J]. *Progress in Aerospace Sciences*, 1998, 34 (5): 257-345.
- [3] Lang Xuwei, Liu xing. Numerical simulation of icing airfoil and analysis of aerodynamic characteristics [J]. *Aeronautical Computing Technique*, 2015, 2015(05): 82-85.
- [4] Zhou Li, Xu Haojun, Yang Zhe, et al. Numerical simulation of ridge ice shapes on airfoil aerodynamics [J]. *Flight Dynamics*, 2012, 6: 489-493.
- [5] Cao Guangzhou, 迎风表面三维积冰的数学模型与计算方法研究 [Research on Mathematical Model and Calculation Method of Three-dimensional Ice Accumulation on Windward Surface]. Doctoral Dissertation, Nanjing University of Aeronautics and Astronautics, Nanjing, China, 2011. (in Chinese)
- [6] Bergman T L, Incropera F P, DeWitt D P, et al. *Fundamentals of heat and mass transfer*[M]. John Wiley & Sons, 2011.
- [7] Su Changming, 热防冰表面水膜流动换热与冰脊生成的数值研究[Numerical study of ridge ice accretion and heat transfer on water film flow under thermal anti-icing conditions]. Nanjing University of Aeronautics and Astronautics, 2017.(in Chinese)
- [8] Broeren A, Bragg M, Addy H, et al. Effect of High-Fidelity Ice Accretion Simulations on the Performance of a Full-Scale Airfoil Model[C]. 46th AIAA Aerospace Sciences Meeting and Exhibit. 2008: 434.

Copyright Statement

The authors confirm that they, and/or their company or organization, hold copyright on all of the original material included in this paper. The authors also confirm that they have obtained permission, from the copyright holder of any third party material included in this paper, to publish it as part of their paper. The authors confirm that they give permission, or have obtained permission from the copyright holder of this paper, for the publication and distribution of this paper as part of the ICAS proceedings or as individual off-prints from the proceedings.